Wavelet-based Texture Segmentation: Two Case Studies

(last edited 02/15/2004)

1 Introduction

In this set of notes, we illustrate wavelet-based texture segmentation on images from the *Brodatz Textures Database* [1]. We perform two sets of experiments on groups of four texture images each, as shown in Figures 1 and 2, respectively. Each individual texture image has dimensions 320×320. For each set of textures, we use the top halves of Figures 1 and 2 for training wavelet-based models of texture appearances, while all testing is conducted on the bottom halves.

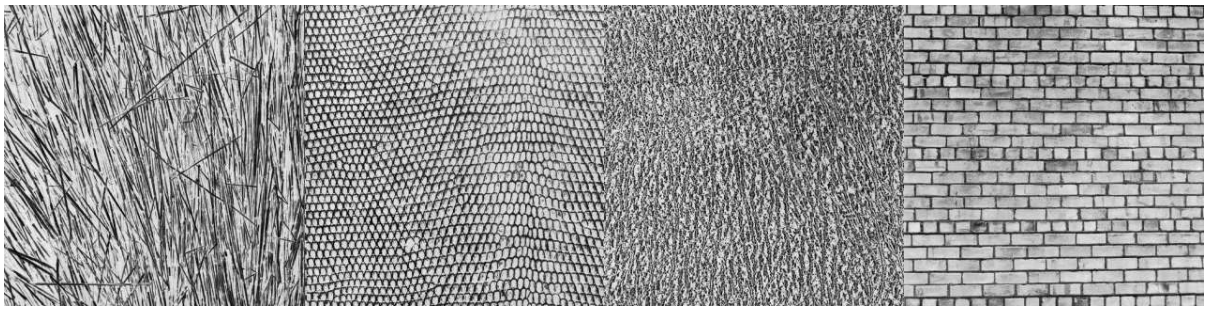

Figure 1: Texture set #1.

Figure 2: Texture set #2.

2 Approach

In this section, we describe our approach to texture segmentation as well as our training of statistical texture-appearance models.

2.1 Training data

In our approach to classifying and segmenting texture images, we choose to analyze 16×16 pixel neighborhoods W. Therefore, for each texture class $\omega \in \{1, \ldots, C\}$, we extract 16×16 subimages W_j^ω, $j \in \{1, \ldots, N\}$, where the origin of each is offset from its nearest neighbor by 4 pixels in both the x and y directions. For example, a 64×64 image generates $13 \times 13 = 169$ subimages, as illustrated in Figure 3 for a small sample texture image. Note that for training images sized 160×320 (top half of individual texture images in Figures 1 and 2), we extract $N = 77 \times 77 = 2849$ individual windows W_j^ω for each texture ω.

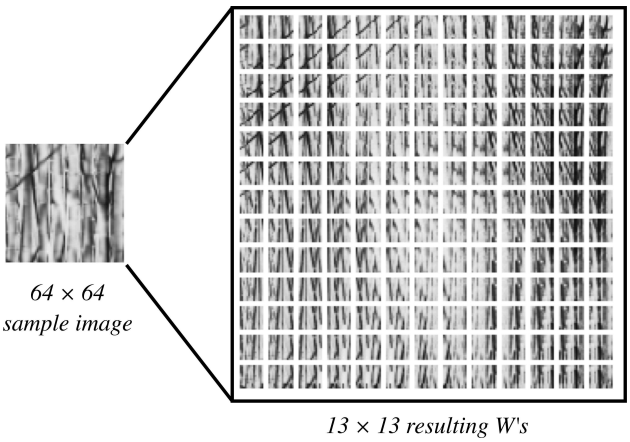

Figure 3: All 16×16 subimages W (offset by 4 pixels) for a 64×64 sample image.

Now, each subimage W_j^ω gives rise to a set of six feature vectors x_{ij}^ω, $i \in \{1, \ldots, 6\}$. As depicted in Figure 4, we first perform a 2-level, 2D Discrete Wavelet Transform (DWT) on W_j^ω. Next, we take the magnitude of the resulting wavelet coefficients. Then, we define x_{ij}^ω as the ith band of the magnitude DWT, where Figure 4 specifies which i corresponds to which band (i.e. LH_1, HL_1, HH_1, LH_2, HL_2 and HH_2). Note that we throw out intensity information in the original image by not including the LL_2 band, since average intensities are not, in general, discriminating for texture images of the type shown in Figures 1 and 2. Finally, we observe that feature vectors x_{1j}^ω, x_{2j}^ω and x_{3j}^ω are of length $8 \times 8 = 64$, while feature vectors x_{4j}^ω, x_{5j}^ω and x_{6j}^ω are of length $4 \times 4 = 16$.

2.2 Statistical texture models

Given the feature vectors x_{ij}^ω, $j \in \{1, \ldots, N\}$, $i \in \{1, \ldots, 6\}$, $\omega \in \{1, \ldots, C\}$, we now want to built histogram probability models for each band i and texture class ω. This requires that we first construct common quantizations of feature spaces i across all texture classes ω. We will derive these feature-specific quantizations using *vector quantization*; see [2] for specifics on vector quantization.

Let $X_i^\omega = \{x_{ij}^\omega\}$ denote all training feature vectors for band i and texture class ω, and let $X_i = \{X_i^\omega\}$ denote all training feature vectors for band i across all texture classes. Then,

$$Z_i^L = VQ(X_i, L) = \{\mu_{ik}\}, \;\; k \in \{1, \ldots, L\} \tag{1}$$

denotes the L-level VQ codebook of prototype vectors $\{\mu_{ik}\}$ trained on X_i, where L is user-defined.

Given the six VQ codebooks Z_i^L, $i \in \{1, \ldots, 6\}$, we can now assign an integer label ℓ_{ij}^ω to every training feature vector x_{ij}^ω:

$$\ell_{ij}^\omega = \arg\min_k d(x_{ij}^\omega, \mu_{ik}) \tag{2}$$

where $d(a, b)$ denotes the Euclidean distance between vectors a and b. Furthermore, let n_{ik}^ω denote the number of vectors in X_i^ω with label $\ell_{ij}^\omega = k$, and let n_i^ω denote the total number of vectors in X_i^ω. Then, we assign the probability of prototype vector μ_{ik} for texture class ω as:

$$P_i^\omega(k) = \frac{n_{ik}^\omega}{n_i^\omega}. \tag{3}$$

The probabilities $H_i^\omega = \{P_i^\omega(k)\}$, $k \in \{1, \ldots, L\}$, define the histogram probability model for feature space (i.e. band) i and texture class ω over quantization Z_i^L.

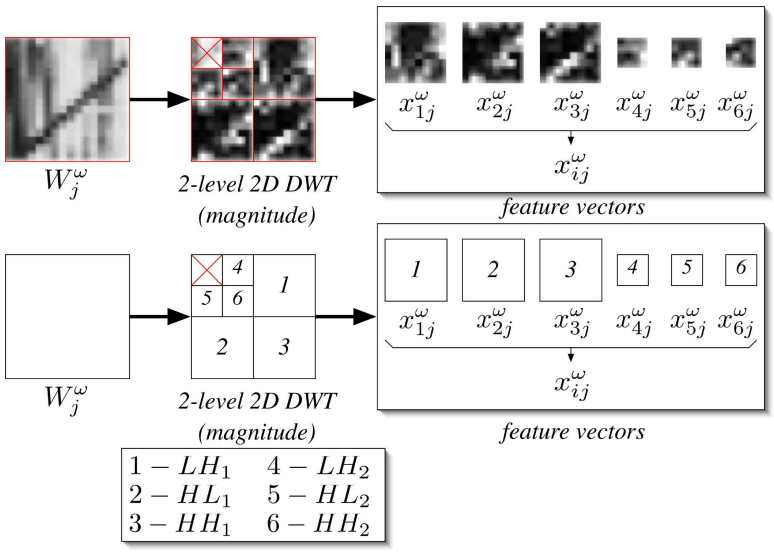

Figure 4: Extraction of feature vectors x_{ij}^ω for subimage W_j^ω.

2.3 Classification

Given the VQ codebooks Z_i^L and histogram models H_i^ω, we are now in position to classify an unknown 16×16 subimage W^t. Let x_i^t, $i \in \{1, \ldots, 6\}$ denote the six feature vectors corresponding to subimage W^t, as in Figure 4), and let ℓ_i^t denote the integer label for x_i^t and VQ codebook Z_i^L, as in equation (2) above. Then, we classify subimage W^t as texture class ω^*, where,

$$\omega^* = \arg\max_\omega \prod_{i=1}^{6} P_i^\omega(\ell_i^t). \tag{4}$$

3 Experiments

In this section, we summarize texture segmentation results for the texture image sets in Figures 1 and 2. Much more detailed results can be found at [3].

3.1 Texture set #1

This set of experiments relates to the $C = 4$ texture images shown in Figure 1; numbering of the textures (from 1 to 4) goes from left to right. The top halves of the texture images were used for training the VQ codebooks Z_i^L and histogram models H_i^ω; the bottom halves of the texture images were used for testing segmentation performance for the resulting models. Values of $L = \{2, 4, 8, 16, 32, 64\}$ were tried; roughly equivalent segmentation performance was achieved for $L = \{16, 32, 64\}$. Therefore, here, we show results only for $L = 16$; additional results are available at [3].

Figure 5 plots the histograms H_i^ω, along with the VQ codebooks Z_i^{16} (below each histogram). Figure 6 illustrates overall segmentation results over test textures with the classification rule as in equation (4). Averaged correct segmentation is approximately 92%; most of the error occurs for texture class $\omega = 1$ for a region that is atypical of the texture image as a whole. Finally, Figure 7 illustrates segmentation results for individual bands i. Note that segmentation performance in Figure 6, when combining probabilities from all bands, is far superior to segmentation results based on individual bands i only.

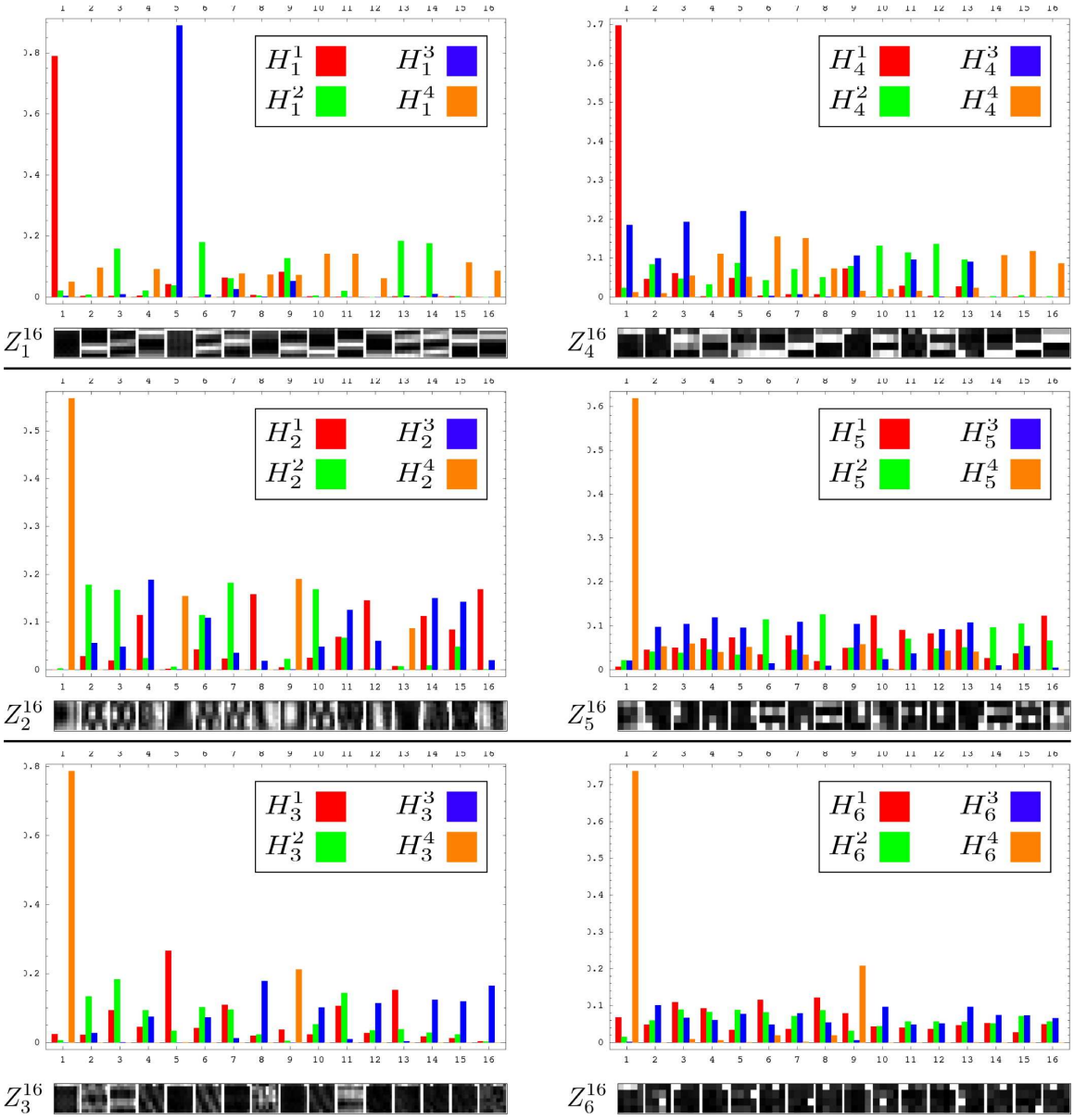

Figure 5: Set #1: VQ codebooks Z_i^{16} and histogram models H_i^ω.

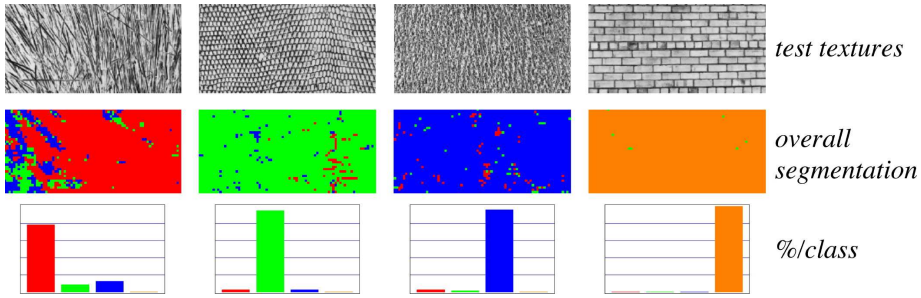

Figure 6: Set #1: Segmentation of test textures. Correct classification is approximately 92%.

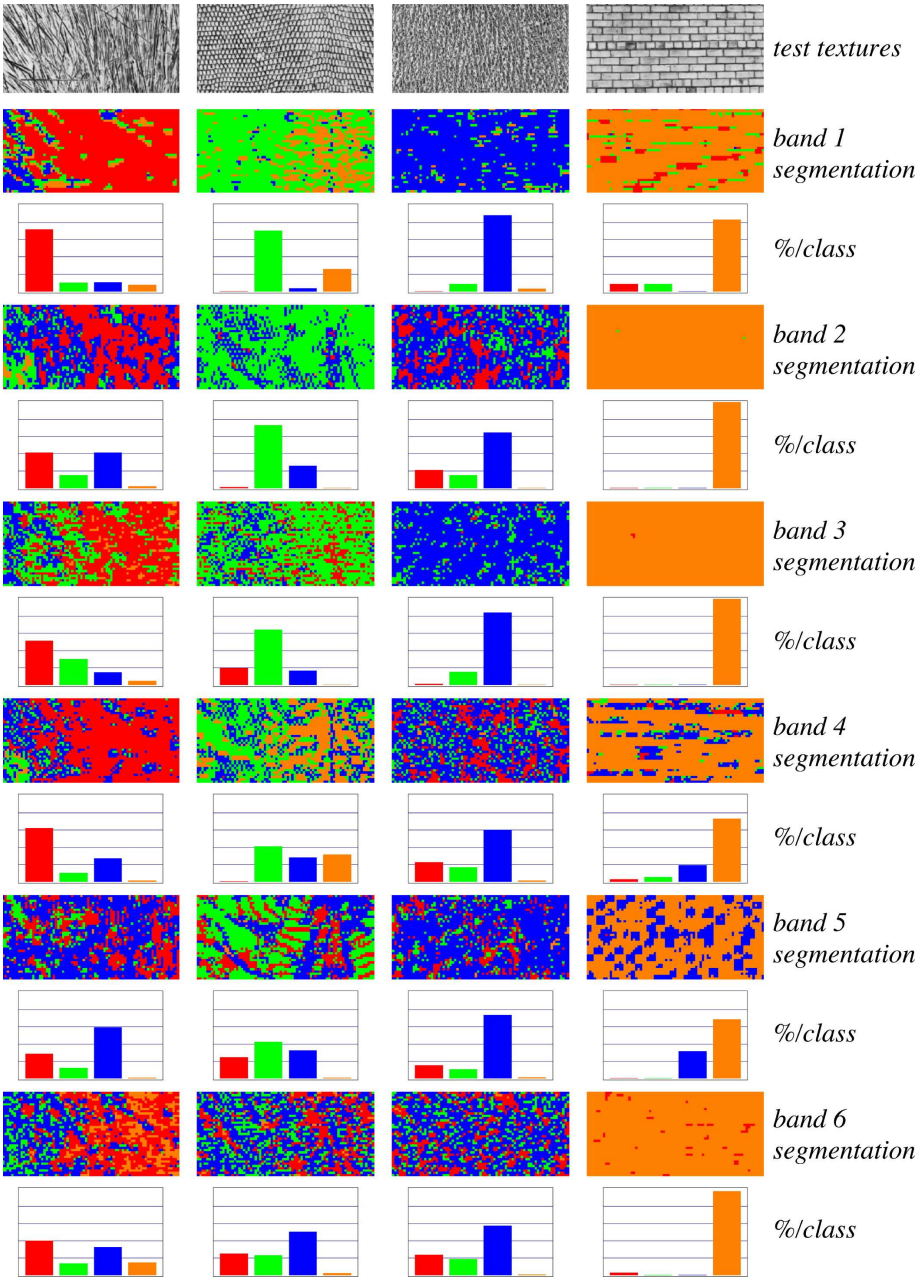

Figure 7: Set #1: Segmentation of test textures based on individual bands i; none of the individual-band segmentations is nearly as good across all texture classes as the results for all bands combined in Figure 6.

3.2 Texture set #2

This set of experiments relates to the $C = 4$ texture images shown in Figure 2; numbering of the textures (from 1 to 4) goes from left to right. The top halves of the texture images were used for training the VQ codebooks Z_i^L and histogram models H_i^ω; the bottom halves of the texture images were used for testing segmentation performance for the resulting models. Values of $L = \{2, 4, 8, 16, 32, 64\}$ were tried; roughly equivalent segmentation performance was achieved for $L = \{16, 32, 64\}$. Therefore, here, we show results only for $L = 16$; additional results are available at [3].

Figure 8 plots the histograms H_i^ω, along with the VQ codebooks Z_i^{16} (below each histogram). Figure 9 illustrates overall segmentation results over test textures with the classification rule as in equation (4). Averaged correct segmentation is approximately 90%; most of the error occurs because of difficulty distinguishing the very similar textures $\omega = 2$ and $\omega = 3$ (two different wood grains). Finally, Figure 10 illustrates segmentation results for individual bands i. Note again that segmentation performance in Figure 9, when combining probabilities from all bands, is far superior to segmentation results based on individual bands i only.

References

[1] *Brodatz Textures Database*, `http://www.ux.his.no/~tranden/brodatz.html`, February, 2004.

[2] *EEL6825*, `http://mil.ufl.edu/~nechyba/__eel6825.f2003/course_materials.html`, Fall, 2003.

[3] *EEL6562*, `http://mil.ufl.edu/~nechyba/eel6562/course_materials.html`, Spring, 2004.

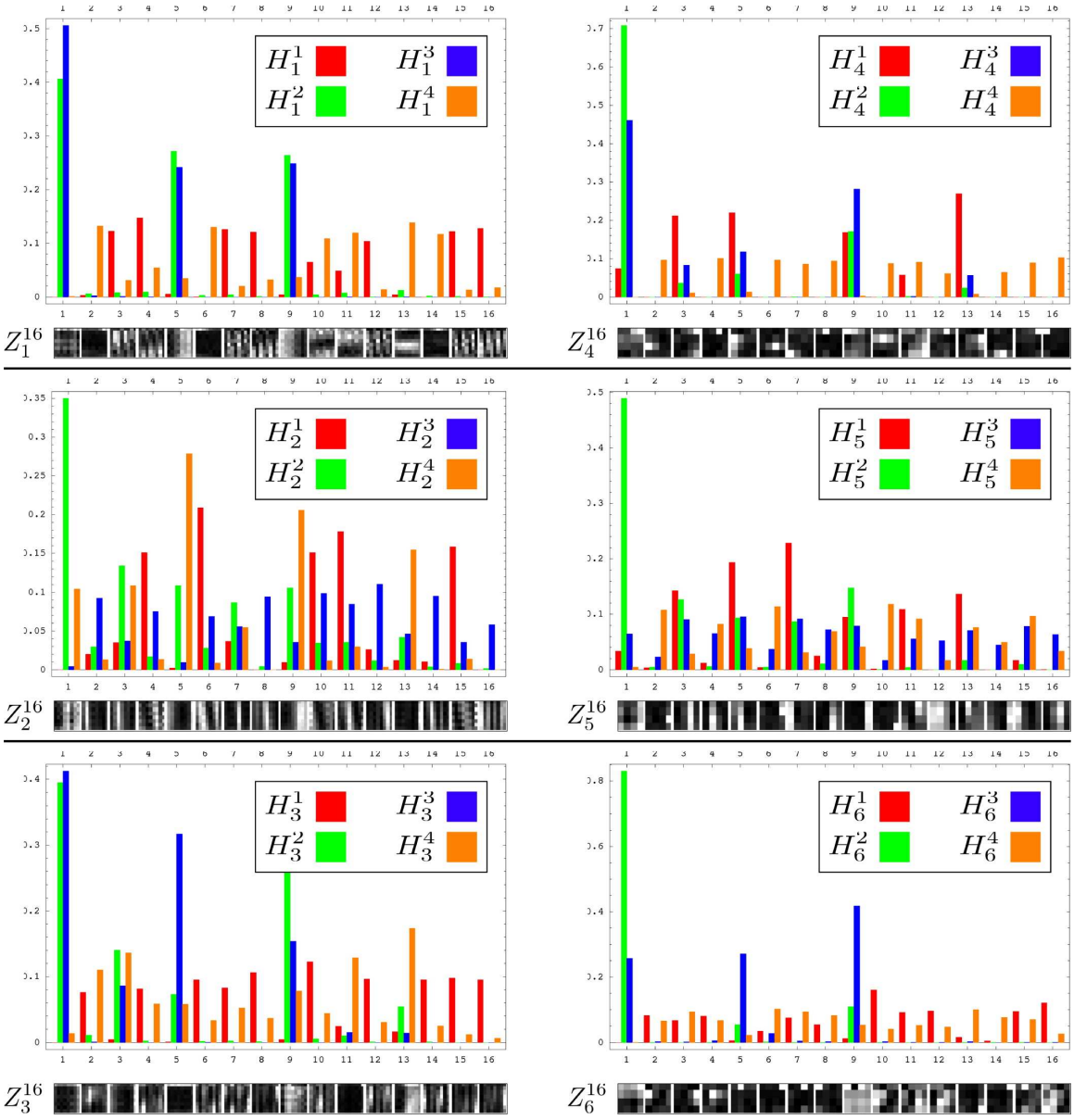

Figure 8: Set #2: VQ codebooks Z_i^{16} and histogram models H_i^ω.

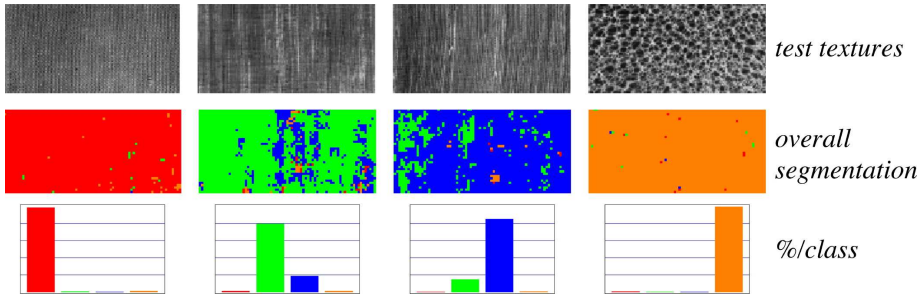

Figure 9: Set #2: Segmentation of test textures. Correct classification is approximately 92%.

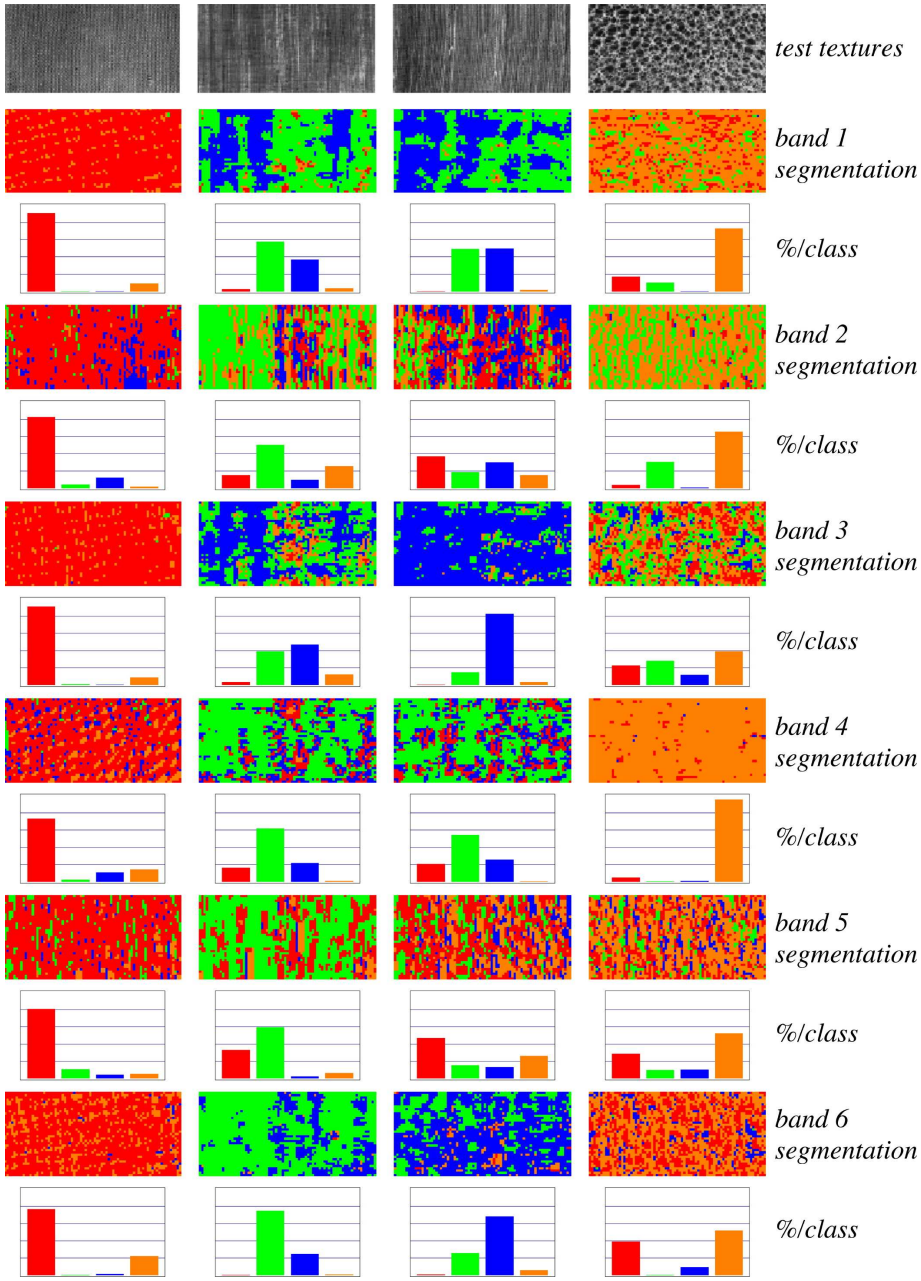

Figure 10: Set #2: Segmentation of test textures based on individual bands i; none of the individual-band segmentations is nearly as good across all texture classes as the results for all bands combined in Figure 9.